Methoden moderner Röntgenphysik II: Streuung und Abbildung

Lecture 24	Vorlesung zum Haupt- oder Masterstudiengang Physik, SoSe 2021		
	G. Grübel, O. Seeck, V. Markmann, F. Lehmkühler, A. Philippi-Kobs, M. Martins		
Location	online		
Date	Tuesdays	12:30 - 14:00	(starting 6.4.)
	Thursdays	8:30 - 10:00	(until 8.7.)

Outline

Part III/1:

Studies on Magnetic Nanostructures

by André Philippi-Kobs

[22.6.] **Ferromagnetism in a Nutshell**

- Introduction to Magnetic Materials
- Magnetic Phenomena
- Magnetic Free Energy
- Perpendicular Magnetic Anisotropy
- Magnetic Domains and Domain Walls

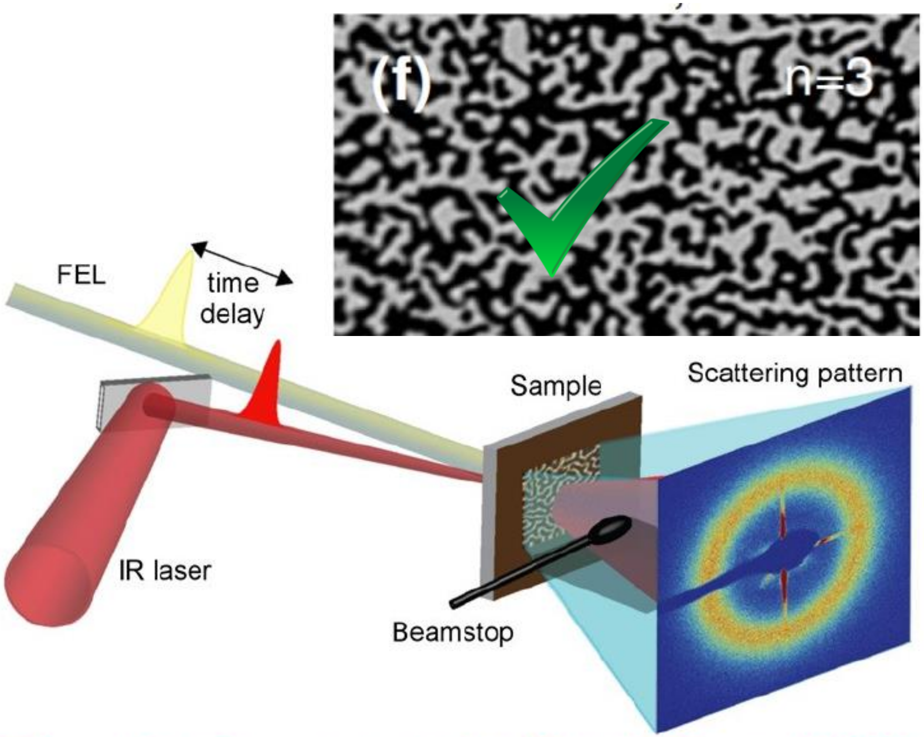

B. Pfau et al., Nature Communications, Vol. 3, 11; DOI:doi:10.1038/ncomms2108 (2012)
L.Müller et al., Rev. Sci. Instrum. 84, 013906 (2013)

[24.6.] **Interaction of Polarized Photons with Ferromagnetic Materials**

- Charge and Spin X-ray Scattering by a Single Electron
- Absorption and Resonant Scattering of Ferromagnets (Semi-Classical and Quantum-Mechanical Concepts)

Outline

Part III/2:

Studies on Magnetic Nanostructures

by André Philippi-Kobs

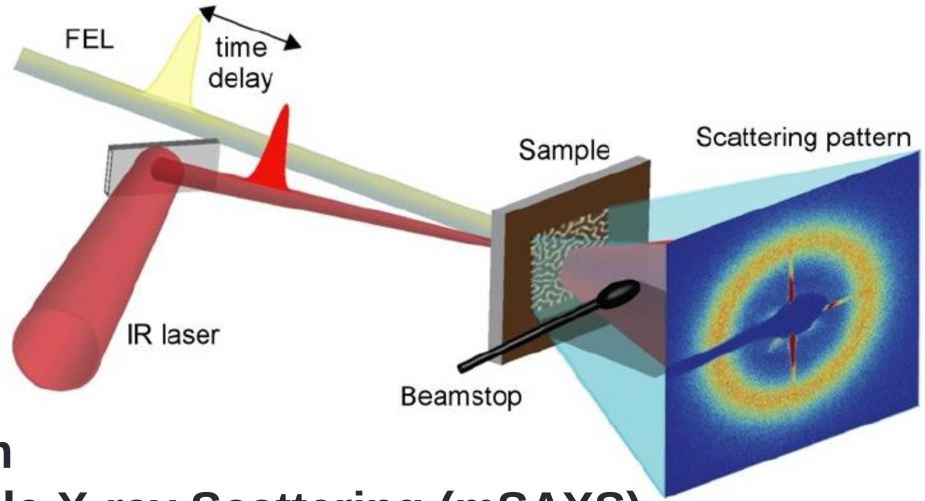

[29.6.] **X-ray Magnetic Circular Dichroism (XMCD) & Resonant Magnetic Small Angle X-ray Scattering (mSAXS)**

- Role of Spin-Orbit Coupling and Exchange Splitting
- Sum Rules
- XMLD and Natural Dichroisms
- mSAXS of Magnetic Domain Patterns

Interaction of **polarized** photons with matter

> X-ray magnetic circular dicroism (XMCD) effect

- Strong ferromagnet:
  one subband is completely filled
- Spin is conserved during transition
- Crystal-field-split-d-states
  (neglect small SOC)

➔ Calculate transition matrix elements for **Spin-Up** electrons & helicity q = ± 1 (RCP and LCP)

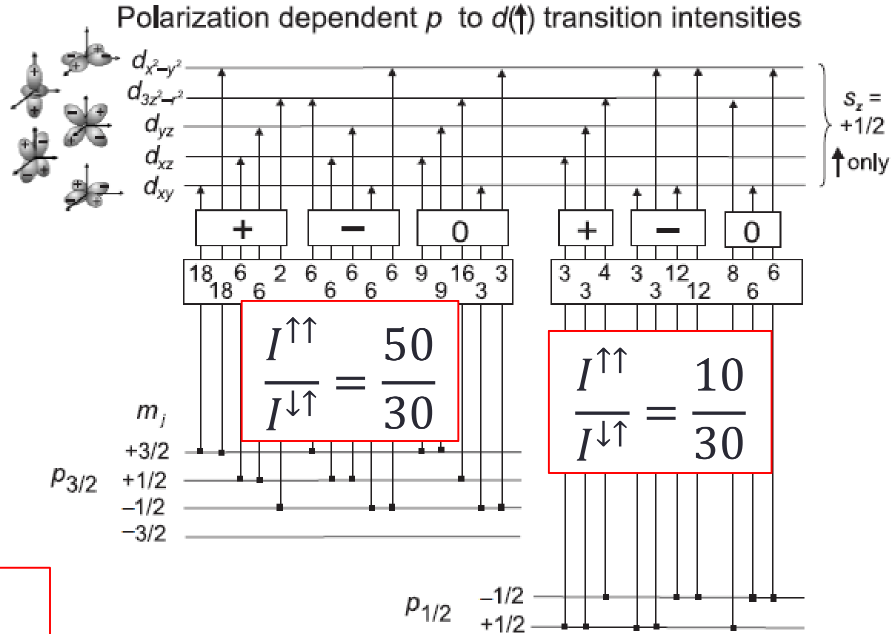

$$\frac{I^{\uparrow\uparrow}}{I^{\downarrow\uparrow}} = \frac{50}{30}$$

$$\frac{I^{\uparrow\uparrow}}{I^{\downarrow\uparrow}} = \frac{10}{30}$$

➔ XMCD: $\boxed{\Delta I = I^{\downarrow\uparrow} - I^{\uparrow\uparrow} \neq 0}$

$$\Delta I_{L_3} = AR^2 \sum_{n,m_j} |\langle d_n, \chi^+ | C_{-1}^{(1)} | p_{3/2}, m_j \rangle|^2 - |\langle d_n, \chi^+ | C_{+1}^{(1)} | p_{3/2}, m_j \rangle|^2 \propto -20$$

$$\Delta I_{L_2} = AR^2 \sum_{n,m_j} |\langle d_n, \chi^+ | C_{-1}^{(1)} | p_{1/2}, m_j \rangle|^2 - |\langle d_n, \chi^+ | C_{+1}^{(1)} | p_{1/2}, m_j \rangle|^2 \propto 20$$

$$-\Delta I_{L3} = \Delta I_{L2}$$

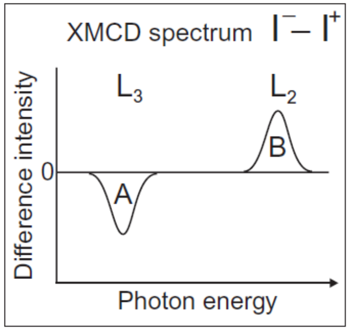

$A = 4\pi^2 \alpha_{\text{fine structure}} \hbar\omega$
R = radial matrix element

L$_3$ and L$_2$ edges have the same XMCD strength

$$\frac{I_{L3,\text{total}}}{I_{L2,\text{total}}} = \frac{80}{40} = 2:1$$

Interaction of **polarized** photons with matter

> X-ray magnetic circular dicroism (XMCD) effect

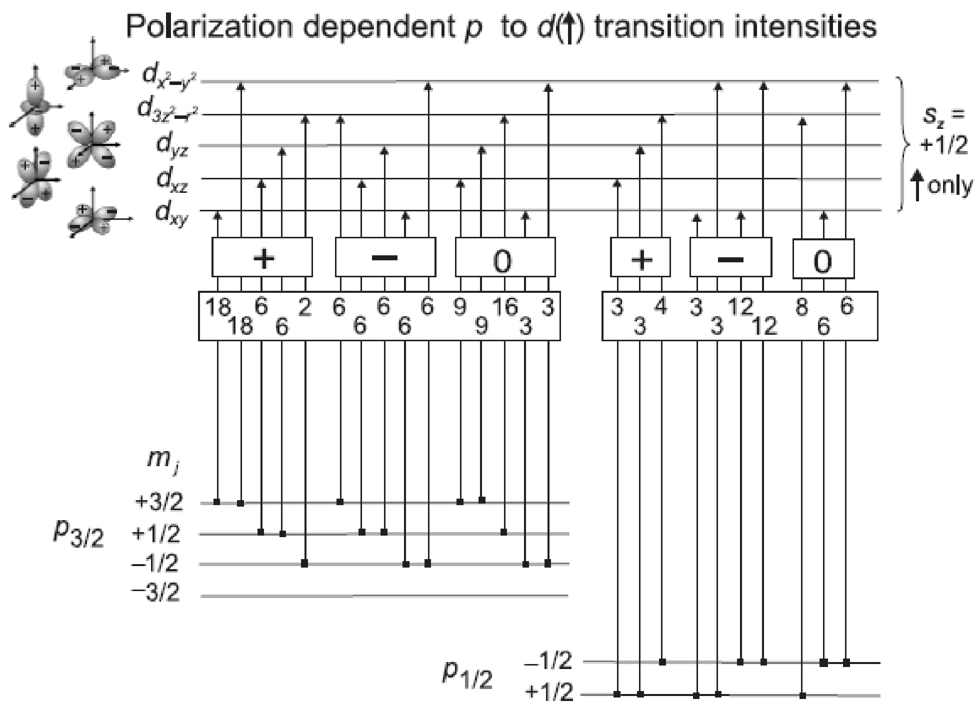

Crystal-field-split d-states

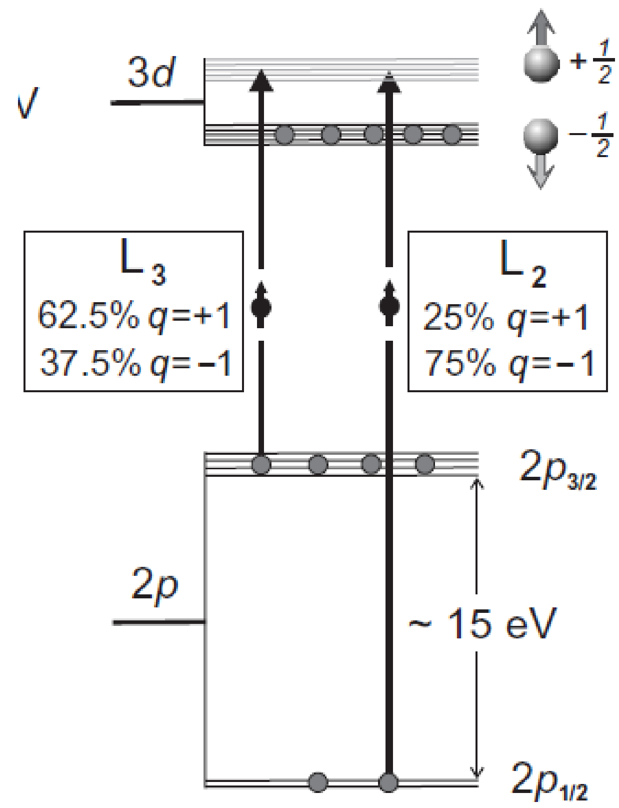

Atomic-exchange-split *d*-states (w/o SOC)

Same results for $I_{L_{3,\text{total}}}\colon I_{L_{2,total}} = 2\colon 1,$

$$\Delta I_{L_{3,total}}\colon \Delta I_{L_{2,total}} = 1\colon -1$$

when using atomic *d*-states (w/o SOC); excercise today

Interaction of **polarized** photons with matter

> X-ray magnetic circular dicroism (XMCD) effect

What is happening in a paramagnet?

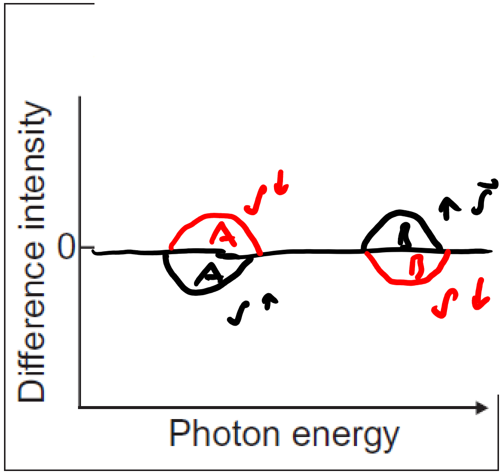

➔ No XMCD

What is happening w/o Spin-Orbit-Coupling for the p-states?

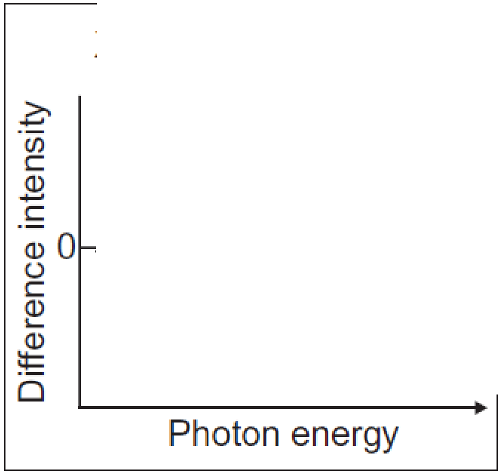

➔ No XMCD

Interaction of **polarized** photons with matter

> X-ray magnetic circular dichroism (XMCD) effect

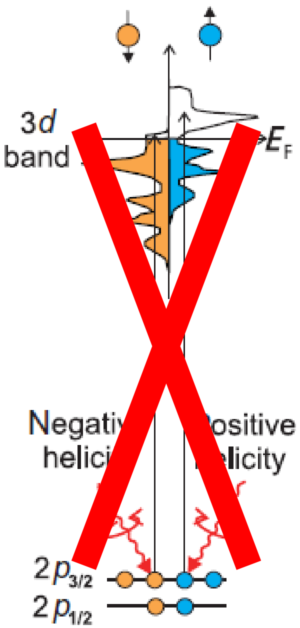

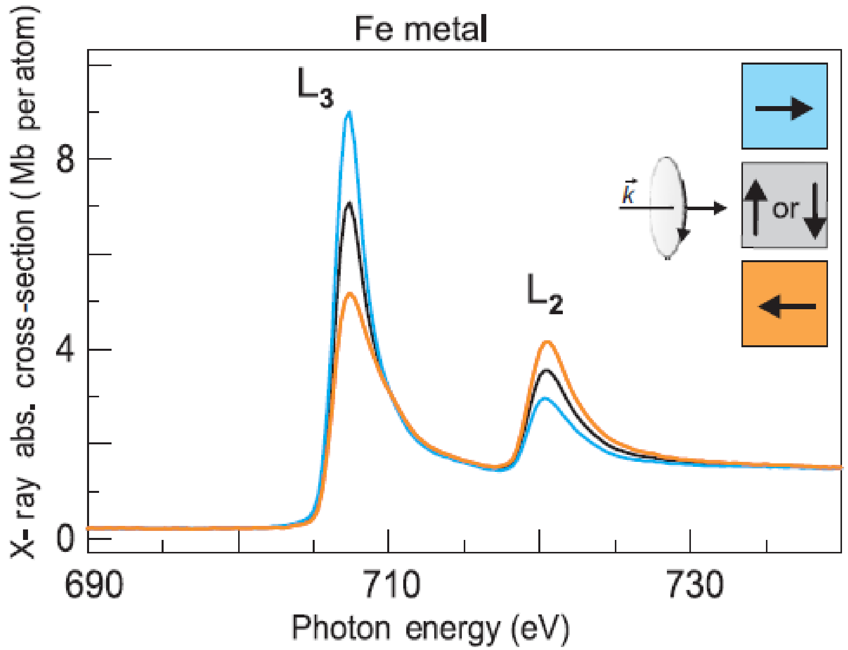

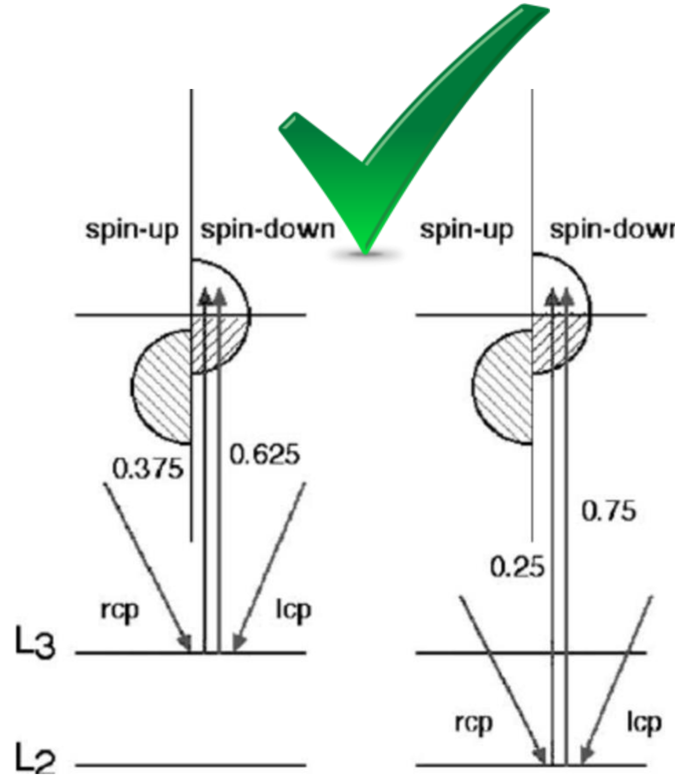

(sketches in textbooks can be misleading!)

$$\Delta I_{\mathrm{XMCD}} \propto \mathbf{M} \cdot \mathbf{L}_{\mathrm{ph}} \propto \cos\theta, \qquad \theta \measuredangle (\mathbf{M}, \mathbf{L}_{\mathrm{ph}})$$

Interaction of **polarized** photons with matter

- (Orientation averaged) Sum rule $$\langle I \rangle = \frac{1}{3}\left(I_\alpha^{-1} + I_\alpha^{0} + I_\alpha^{+1}\right) \qquad (\alpha = z)$$

Density of d-states at E_F $$\sigma^{\mathrm{abs}} = 4\pi^2 \frac{e^2}{4\pi\epsilon_0\hbar c}\, \hbar\omega\, |\langle b|\,\boldsymbol{\epsilon}\cdot\boldsymbol{r}|a\rangle|^2\, \delta[\hbar\omega - (E_b - E_a)]\, \rho(E_b)$$

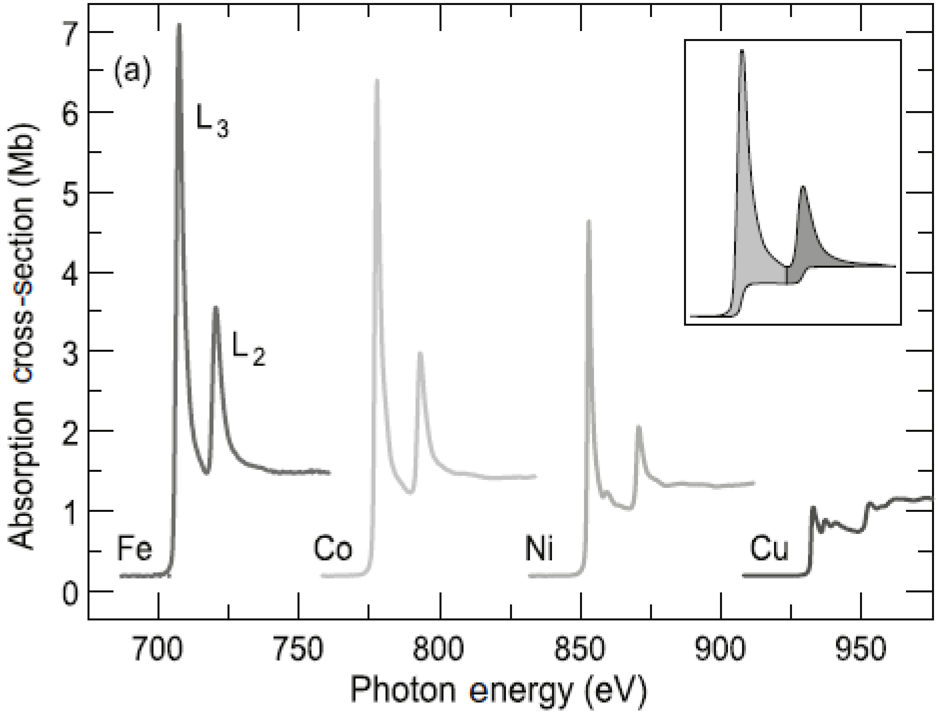

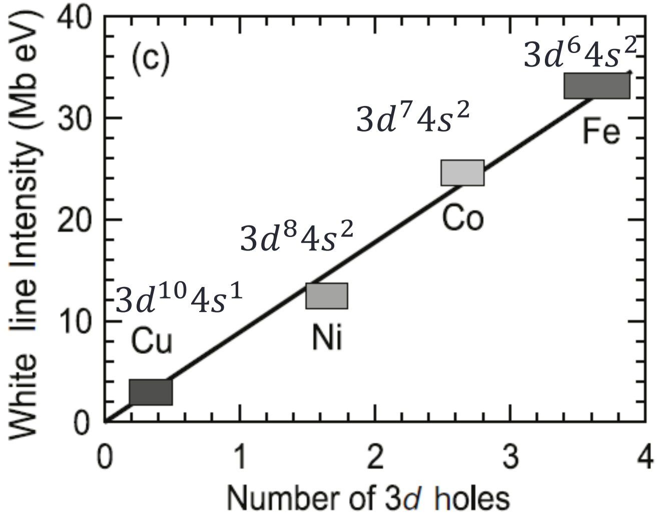

$$D_d(E_\mathrm{F}) = \frac{\langle I_{L_3} + I_{L_2}\rangle}{C} \quad \text{with } C = AR^2\frac{L}{3(2L+1)}$$

Orientation averaged refers to polycrystalline samples, such that anisotropic charge and spin order is eliminated

Interaction of **polarized** photons with matter

- Sum rules

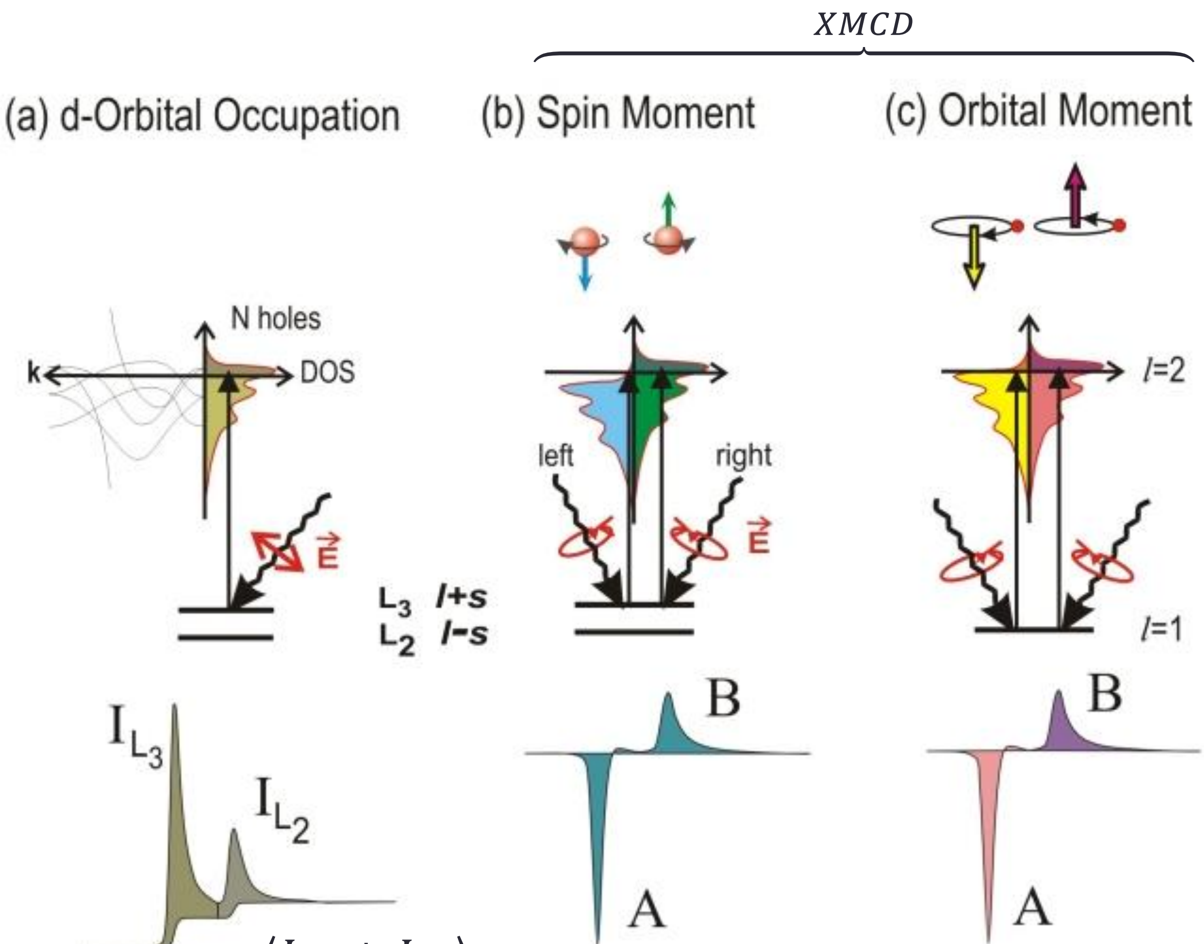

$$D(E_\mathrm{F}) = \frac{\langle I_{L_3} + I_{L_2} \rangle}{C}$$

SOC ~50 meV
for *d*-electrons

$$|\mathbf{m}_{\text{orbital}}| \ll |\mathbf{m}_{\text{spin}}|$$

Spin moment

$$|\mathbf{m}_{\text{spin}}| = \frac{\mu_B \langle -A + 2B \rangle}{C}$$

Angular moment

$$|\mathbf{m}_{\text{orbital}}| = \frac{2\mu_\mathrm{B} \langle A + B \rangle}{3C}$$

Interaction of **polarized** photons with matter

> <u>Application of XMCD</u>

J. Appl. Phys. 67 (9), 1 May 1990

DORIS II at HASYLAB, DESY, Hamburg.

Spin-dependent x-ray absorption in Co/Pt multilayers and $Co_{50}Pt_{50}$

G. Schütz, R. Wienke, and W. Wilhelm
Fak. f. Physik, TU München, D-8046 Garching, Federal Republic of Germany
W. B. Zeper
Philips Research Laboratories, P.O. Box 80.000, 5600 JA Eindhoven, The Netherlands
H. Ebert
Siemens AG, ZFE ME TPH 11, Postfach 3220, D-8520 Erlangen, Federal Republic of Germany
K. Spörl
Institut für Angew. Physik, University of Regensburg, Federal Republic of Germany

The spin dependence of $L_{2,3}$ absorption in 5*d* atoms oriented in a ferromagnetic matrix contains information on the spin density of the empty *d*-projected states of the absorbing atom. Spin-dependent absorption spectroscopy using circularly polarized synchrotron radiation was applied to study the polarization of the Pt atoms in the binary alloy $Co_{50}Pt_{50}$ and Pt/Co layered structures, which are promising candidates for magneto-optical recording. The spin-dependent absorption signals for vapor-deposited 250(4 Å Co + 18 Å Pt) and 250(6 Å Co + 18 Å Pt) multilayers indicate a ferromagnetic coupling on Pt and Co atoms with a significant Pt polarization. This is reduced on average by about 60% with respect to the Pt polarization in the $Co_{50}Pt_{50}$ alloy. The experimental results are discussed on the basis of spin-polarized band-structure calculations.

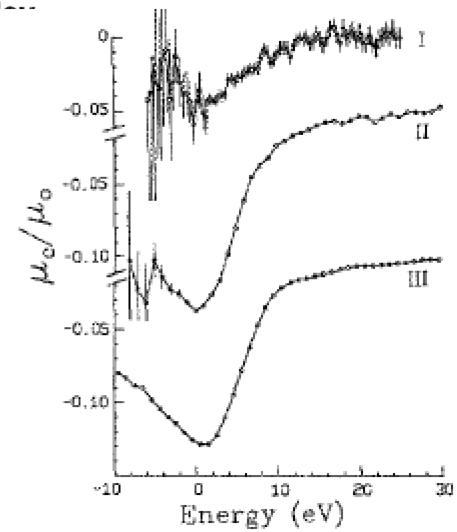

XMCD, CoPt

XMCD FePt

$$|\vec{m}_s|_{\mathrm{Pt}}^{\mathrm{CoPt}} = 0.35\mu_B/\text{atom}$$
$$|\vec{m}_s|_{\mathrm{Pt}}^{\mathrm{FePt}} = 0.08\mu_B/\text{atom}$$

‘Historic’ example at hard x-ray energies (~11.5 keV) corresponding to the Platinum $L_{2,3}$ edge

Interaction of **polarized** photons with matter

> X-ray magnetic circular dicroism (XMCD) effect

(Most important) take-home messages:

- Interaction of ferromagnet and EM wave described by time-dependent pertubation theory
- Transition matrix element with polarization dependent dipole operator describes the possible electronic transitions (dipole selection rules)
- Dipole selection rules:

$$\begin{aligned}\Delta l &= l' - l = \pm 1\\ \Delta m_l &= m_l' - m_l = q = 0, \pm 1\\ \Delta s &= s' - s = 0\\ \Delta m_s &= m_s' - m_s = 0\end{aligned}$$

q = helicity of light
(i.e., polarizations lin., RCP, LCP)

- Calculation of all possible 2p-3d transitions for a ferromagnet where (a) one 3d-subband (↑) is completely filled and (b) the p-states are spin-orbit split

➔ XMCD-effect: The absorption at the L_3 ($2p_{3/2}$-$3d^{\downarrow}$) and L_2 edge ($2p_{1/2}$-$3d^{\downarrow}$) strongly depends on the helicity of the EM wave

DESY

Interaction of **polarized** photons with matter

> XMCD and XMLD effect

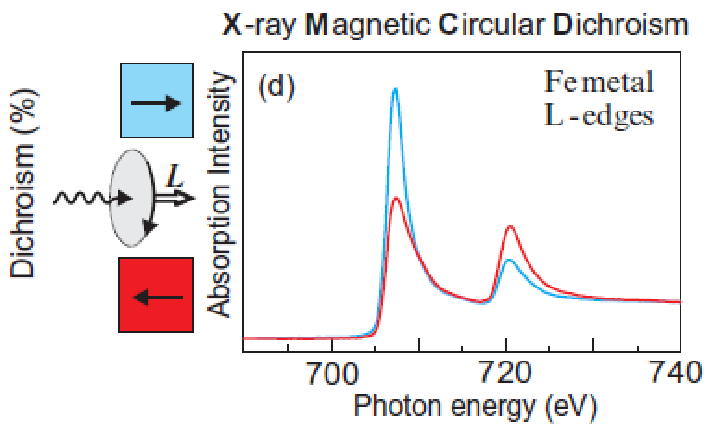

X-ray "magnetic" dichroism is due to spin alignment and the spin–orbit coupling.

– X-ray magnetic circular dichroism – XMCD – arises from *directional* spin alignment. The effect is parity even and time odd.

– X-ray magnetic linear dichroism – XMLD – arises from a charge anisotropy induced by *axial* spin alignment. The effect is parity even and time even.

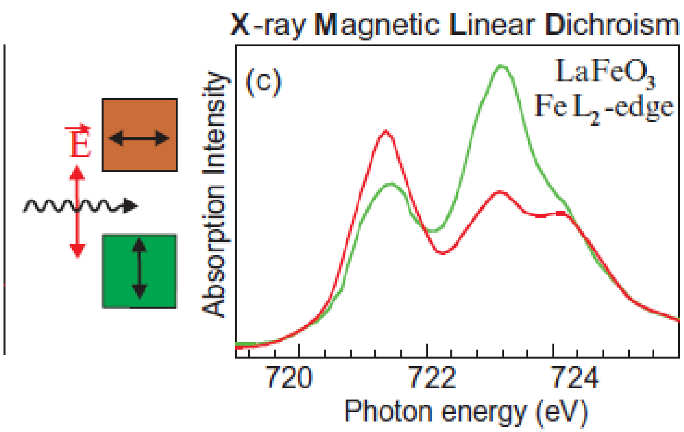

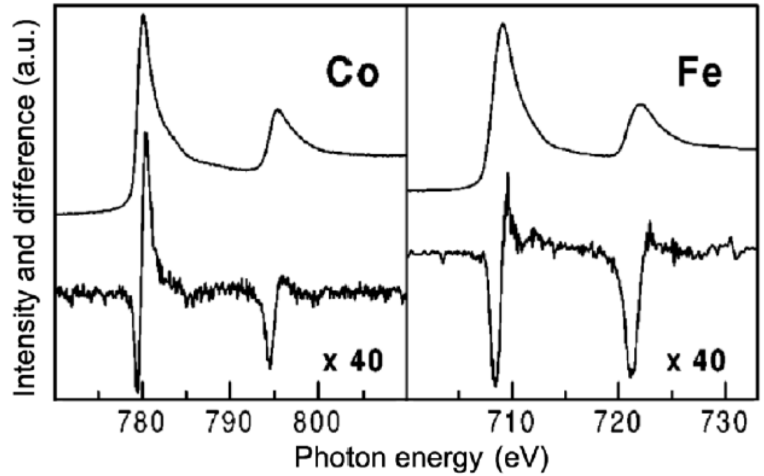

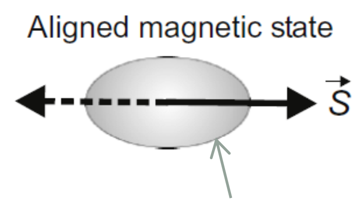

anisotropic charge distribution Due to SOC

Interaction of **polarized** photons with matter

> XNLD and XNCD effect

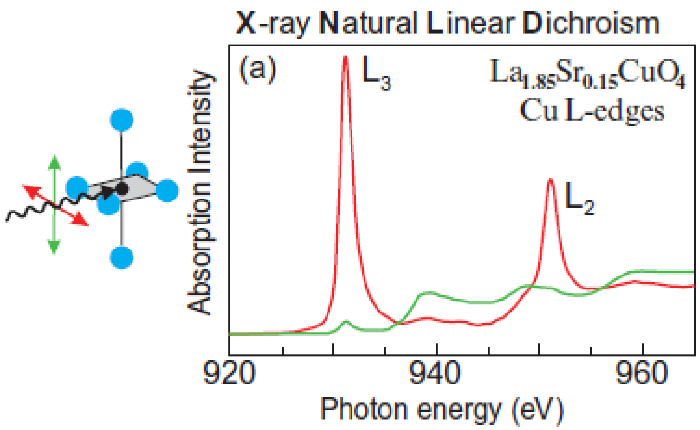

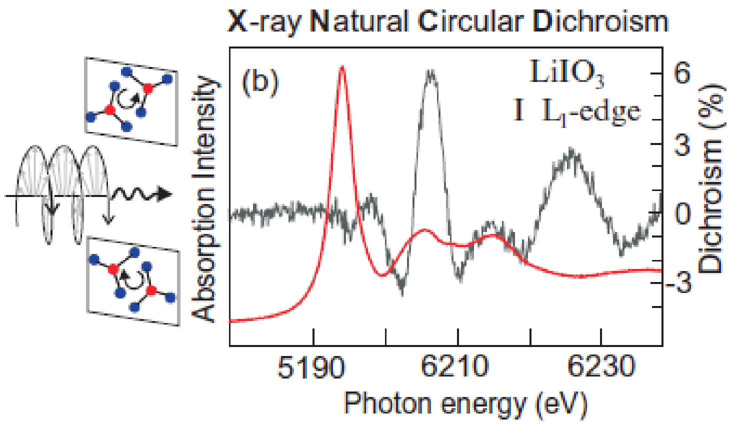

X-ray "natural" dichroism refers to the absence of spin alignment.

– X-ray natural linear dichroism – XNLD – is due to an anisotropic charge distribution. The effect is parity even and time even.
– X-ray natural circular dichroism – XNCD – may be present for anisotropic charge distributions that lack a center of inversion. The effect is parity odd and time even.

Interaction of **polarized** photons with matter

> From Absorption to Resonant Scattering (exp. approach):

$f'' = -(k/4\pi)\, \sigma_a\, (E)$

Measure absorption cross-section for both helicities

Kramers-Kronig relation

f'

$$\sigma_{\text{scattering}} = f^2$$
$$= [Z + f'(\omega, \boldsymbol{\varepsilon})]^2 + [f''(\omega, \boldsymbol{\varepsilon})]^2$$

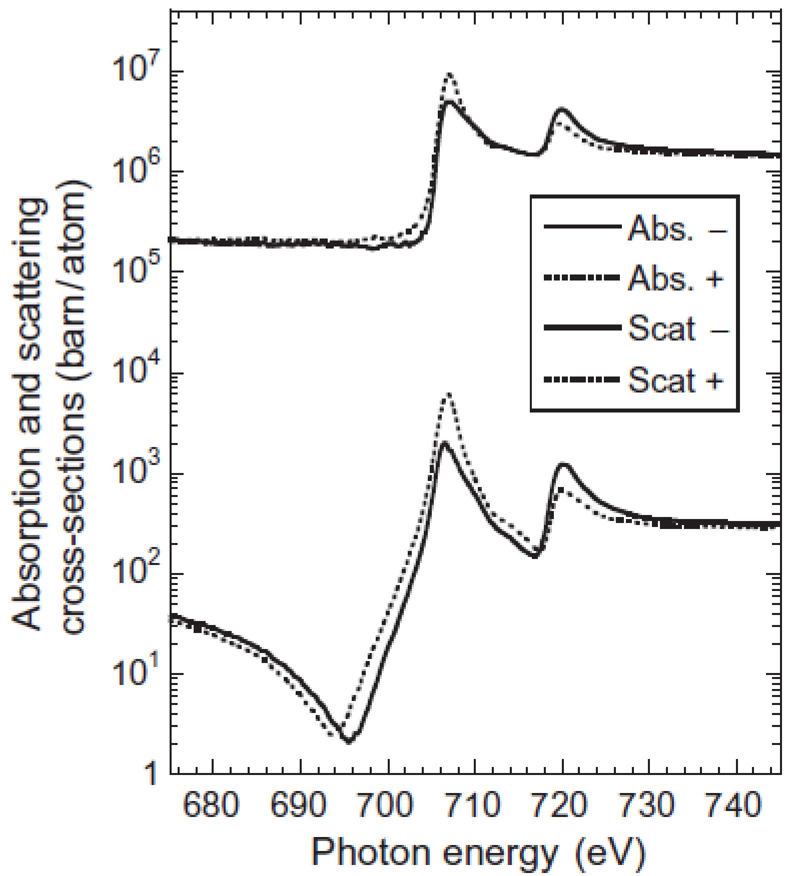

Interaction of **polarized** photons with matter

> Resonant scattering (qm concept): 2. Term of Fermi's Golden rule in dipole approx.

$$T_{if} = \frac{2\pi}{\hbar}\left| \langle f|\mathcal{H}_{\text{int}}|i\rangle + \sum_n \frac{\langle f|\mathcal{H}_{\text{int}}|n\rangle\langle n|\mathcal{H}_{\text{int}}|i\rangle}{\varepsilon_i - \varepsilon_n}\right|^2 \delta(\varepsilon_i - \varepsilon_f)\rho(\varepsilon_f) \qquad \sigma = \frac{T_{if}}{\Phi_0}$$

$\downarrow$ Dipol approximation etc. (as done for absorption term)

$$\frac{\hbar^2\omega^4}{c^2}\,\alpha_{\text{f}}^2 \left| \sum_n \frac{\langle a|\boldsymbol{r}\cdot\boldsymbol{\epsilon}_2^*|n\rangle\langle n|\boldsymbol{r}\cdot\boldsymbol{\epsilon}_1|a\rangle}{(\hbar\omega - E_R^n) + \text{i}(\Delta_n/2)}\right|^2$$

Δ_n: line width of intermediate states

$\downarrow$ J. P. Hannon et al., Phys. Rev. Lett **61**, 1245 (1988)

$$\begin{aligned}\langle a|\boldsymbol{r}\cdot\boldsymbol{\epsilon}_2^*|n\rangle\langle n|\boldsymbol{r}\cdot\boldsymbol{\epsilon}_1|a\rangle = \frac{\mathcal{R}^2}{2}\Big[&(\boldsymbol{\epsilon}_2^*\cdot\boldsymbol{\epsilon}_1)\left\{|C_{+1}|^2 + |C_{-1}|^2\right\} \\ &+ \text{i}(\boldsymbol{\epsilon}_2^*\times\boldsymbol{\epsilon}_1)\cdot\hat{\boldsymbol{m}}\left\{|C_{-1}|^2 - |C_{+1}|^2\right\} \\ &+ (\boldsymbol{\epsilon}_2^*\cdot\hat{\boldsymbol{m}})(\boldsymbol{\epsilon}_1\cdot\hat{\boldsymbol{m}})\left\{2|C_0|^2 - |C_{-1}|^2 - |C_{+1}|^2\right\}\Big]\end{aligned}$$

Interaction of **polarized** photons with matter

> Resonant scattering: 2. Term of Fermi's Golden rule in dipole approximation

$$T_{if} = \frac{2\pi}{\hbar}\left| \langle f|\mathcal{H}_{\text{int}}|i\rangle + \sum_n \frac{\langle f|\mathcal{H}_{\text{int}}|n\rangle\langle n|\mathcal{H}_{\text{int}}|i\rangle}{\varepsilon_i - \varepsilon_n}\right|^2 \delta(\varepsilon_i - \varepsilon_f)\rho(\varepsilon_f)$$

with $\sigma = \dfrac{T_{if}}{\Phi_0}$ and $\sigma_{\text{scattering}} = f^2$

➔ The *elastic resonant magnetic scattering factor* in units [number of electrons] is given by

$$f(\omega,\boldsymbol{\varepsilon}_1) = \frac{\hbar\omega^2\alpha_f\mathcal{R}^2}{2cr_0}\left[\underbrace{(\epsilon_2^*\cdot\epsilon_1)\,G_0}_{\text{charge}} \boxed{+\,\mathrm{i}\underbrace{(\epsilon_2^*\times\epsilon_1)\cdot\hat{m}\,G_1}_{\text{XMCD}}} + \underbrace{(\epsilon_2^*\cdot\hat{m})(\epsilon_1\cdot\hat{m})\,G_2}_{\text{XMLD}}\right]$$

$$\boxed{G_1 = \sum_n \frac{|\langle a|C_{-1}^{(1)}|n\rangle|^2 - |\langle a|C_{+1}^{(1)}|n\rangle|^2}{(\hbar\omega - E_R^n) + \mathrm{i}(\Delta_n/2)}}$$

for circularly polarized light

$$\mathrm{i}\left[(\boldsymbol{\epsilon}^{\pm})^* \times \boldsymbol{\epsilon}^{\pm}\right] = \mp\,\mathbf{e}_z$$

Charge scattering/XNLD

$$G_0 = \sum_n \frac{|\langle a|C_{+1}^{(1)}|n\rangle|^2 + |\langle a|C_{-1}^{(1)}|n\rangle|^2}{(\hbar\omega - E_R^n) + \mathrm{i}(\Delta_n/2)}$$

XMLD

$$G_2 = \sum_n \frac{2|\langle a|C_0^{(1)}|n\rangle|^2 - |\langle a|C_{-1}^{(1)}|n\rangle|^2 - |\langle a|C_{+1}^{(1)}|n\rangle|^2}{(\hbar\omega - E_R^n) + \mathrm{i}(\Delta_n/2)}$$

mSAXS of magnetic domain patterns

Note: HERE: $2\theta =$ total scattering angle
This is a non-standard nomenclature; usually the scattering angle is called θ! [for SAXS]

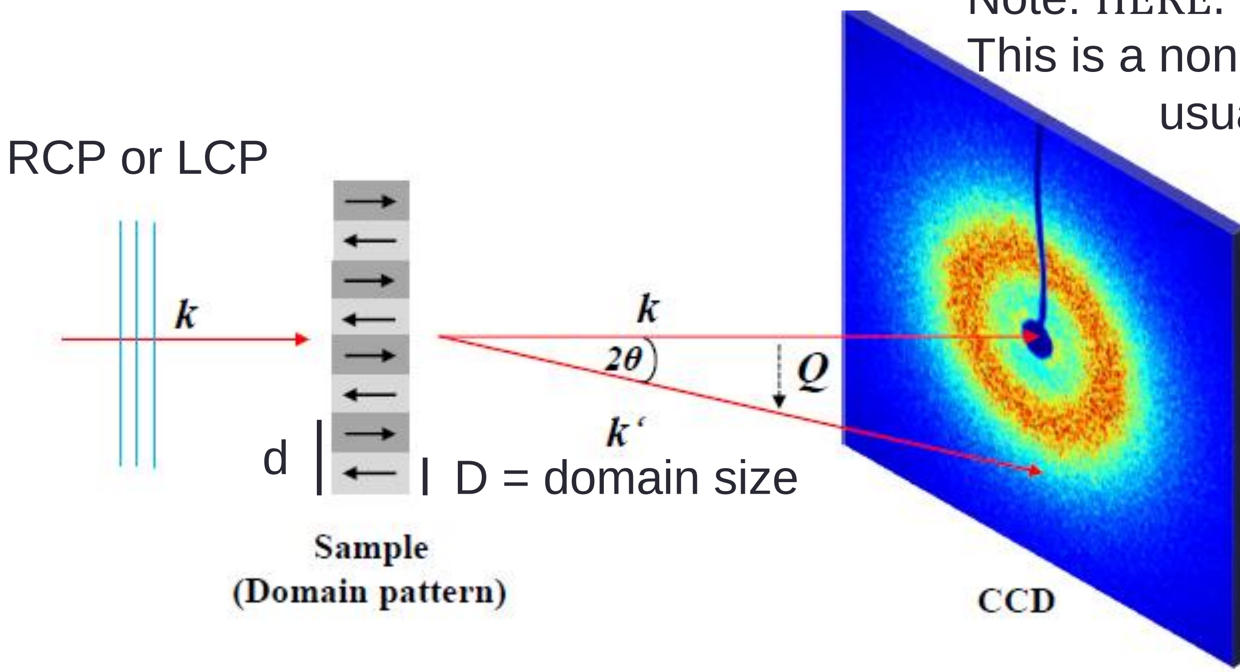

“magnetic grating/lattice“ = stripe domain pattern with equal domain size *D* (periodicity of *d* = 2*D*)

➔ Scattering factor $f_m = M_z F^m$ varies in x-direction due to XMCD effect & alternating M_z

$$f_m(x) \propto \underbrace{f_m^0}_{\text{unit cell}} \otimes \underbrace{\sum_n \delta(x - nd)}_{\text{lattice}}$$

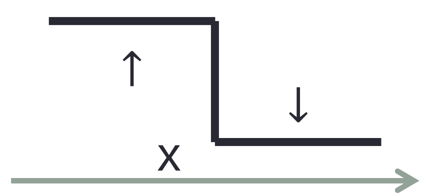

Domain wall thickness =0

mSAXS of magnetic domain patterns

Scattering amplitude (Fourier transform of scattering factor):

$$A(Q) = FT\big(f_m(x)\big) \propto \underbrace{\tilde{f}(Q)}_{\text{unit cell}} \underbrace{\textstyle\sum_n e^{-iQnd}}_{\text{lattice sum}}$$ (for a regular magnetic lattice, e.g., stripes)

2θ = full scattering angle!

With scattering vector = momentum transfer $Q = k - k' = \frac{4\pi}{\lambda} \cdot \sin\theta$ (1)

Scattering intensity:

N_d : ½ number of domains

$$I(Q) = |A(Q)|^2 \propto \begin{cases} |\tilde{f}(Q)|^2 \cdot N_d^2 & \text{for } e^{iQnd} = 1 \\ \sim 0 & \text{else} \end{cases}$$

intensity for $Q \cdot d = 2\pi \cdot n' \underset{n'=1}{\Longrightarrow} Q = \frac{2\pi}{d}$ (2)

(1) & (2): $\sin\theta = \lambda/2d$

for typical domain periodicities of $d = 200\text{nm}$ and $\lambda_{\text{Co}, L\text{-edge}} = 1.5\text{nm}$:

$2\theta = 0.43°$, i.e., first maximum at 4.5 mm distance from $Q = 0$
for sample-detector distance of 600 mm

mSAXS of magnetic domain patterns

What happens when the magnetic domains are disordered?

The discrete Fourier sum (lattice)

$$I(Q) = |FT(f_m(x))|^2 \propto \left| \underbrace{\tilde{f}(Q)}_{\text{unit cell}} \underbrace{\sum_n e^{-iQnd}}_{\text{lattice sum}} \right|^2$$

becomes an integral over the magnetic structure

$$I(\mathbf{q}) = \left| \int_V f_m(\mathbf{r}) \exp(i\mathbf{Q}\cdot\mathbf{r})\, d\mathbf{r} \right|^2 = \left| \int_V \mathbf{e}_z \cdot \mathbf{M}(\mathbf{r})\, G_1 \exp(i\mathbf{Q}\cdot\mathbf{r})\, d\mathbf{r} \right|^2$$

$$I(\mathbf{q}) = \left| \int_V M_z(\mathbf{r})\, G_1 \exp(i\mathbf{Q}\cdot\mathbf{r})\, d\mathbf{r} \right|^2$$

Good assumption: Homogeneous magnetization along z-direction (through the thickness of the film || **k**)

➔ Measurement of the absolute square of the Fourier transform of the z-component of magnetization pattern.
(The detection of in-plane components requires tilting of the sample with respect to **k**)

mSAXS of magnetic domain patterns

Consideration of domain wall width (1D model)

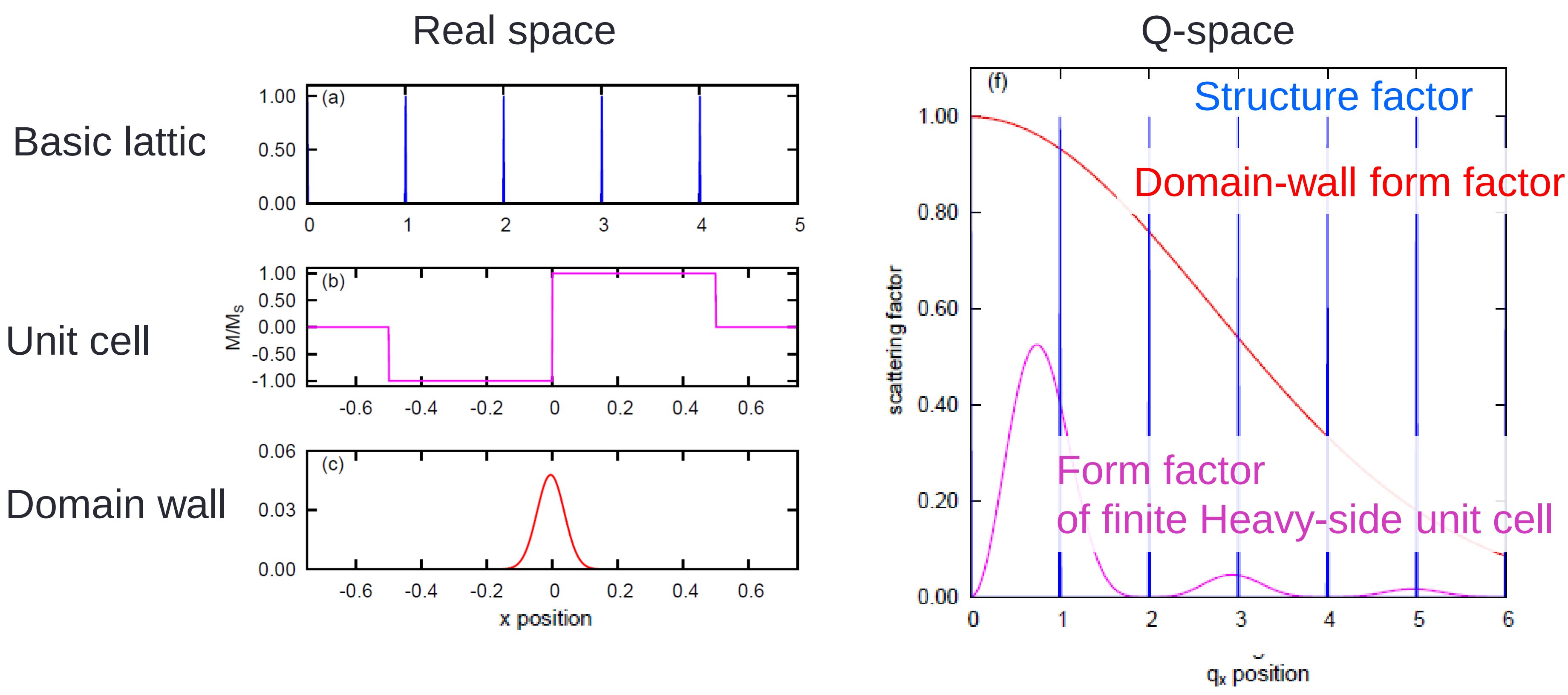

mSAXS of magnetic domain patterns

Consideration of domain wall size (1D model)

Real space

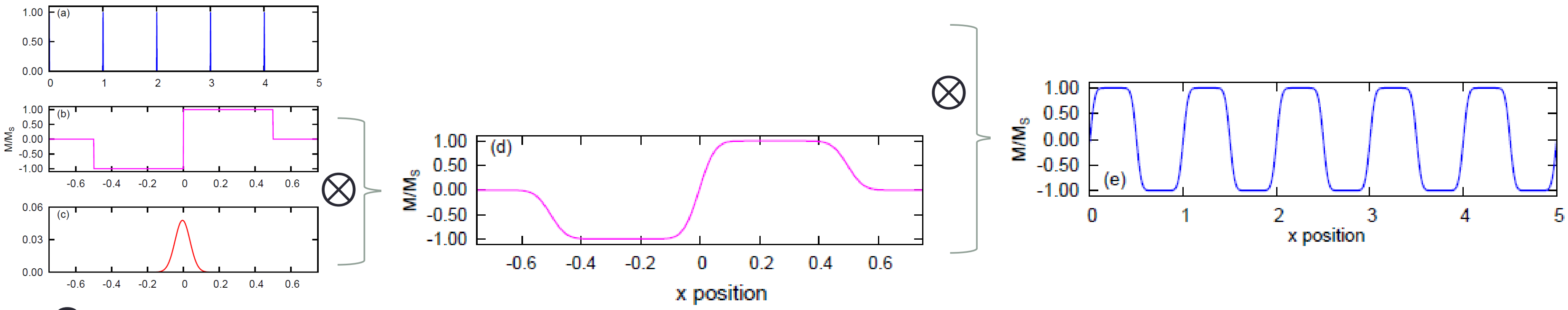

Q-space

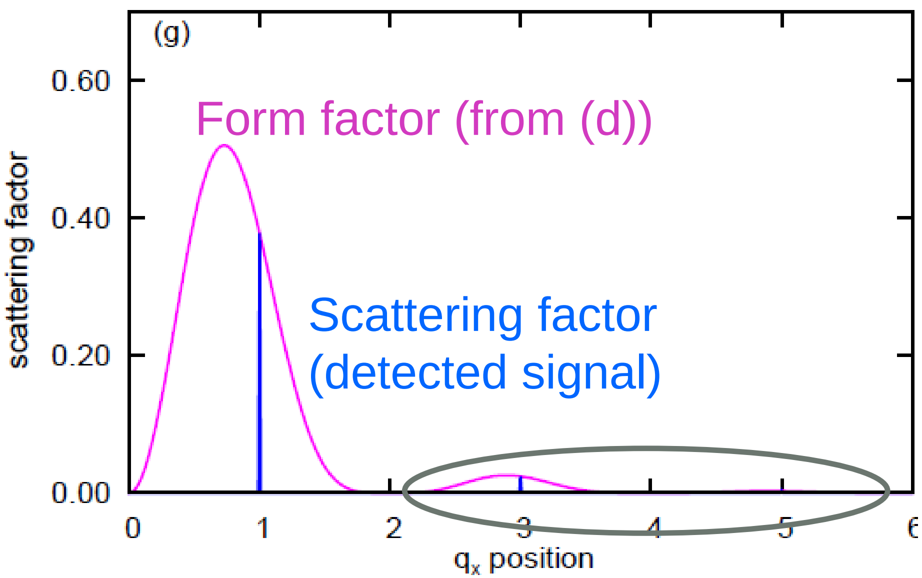

Note: Finite domain-wall width ℓ decreases the peak intensities $\propto e^{-\ell^2 q^2}$, i.e., like a Debye-Waller factor [there: Δr caused by thermal movement].

➔ Strong impact of changes in ℓ on signal strength

mSAXS of magnetic domain patterns

Consideration of domain size distribution(in 1D)

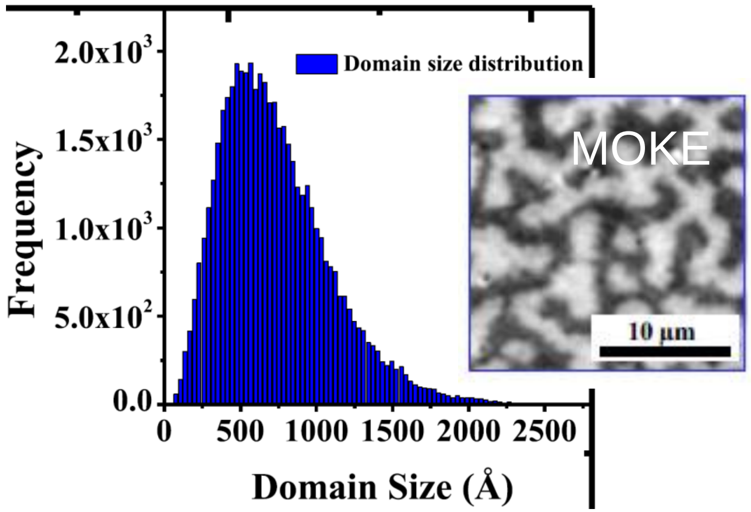

Size distribution follows
Gamma distribution (for large domains)

$$g(x) = \frac{x^{k-1}\exp\left(-\frac{x}{\vartheta}\right)}{\vartheta^k \Gamma(k)}, \quad x > 0$$

Can we reproduce the shape of the radial scattered intensity when assuming a Gamma distribution?

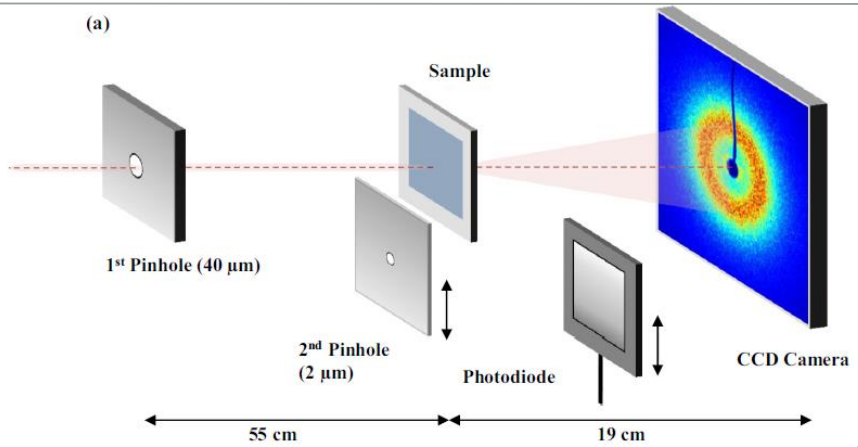

K. Bagschik et al., PRB **94**, 134413 (2016).

mSAXS of magnetic domain patterns

Consideration of domain size distribution(in 1D)

STXM (transmission of CP light) along Co wedge

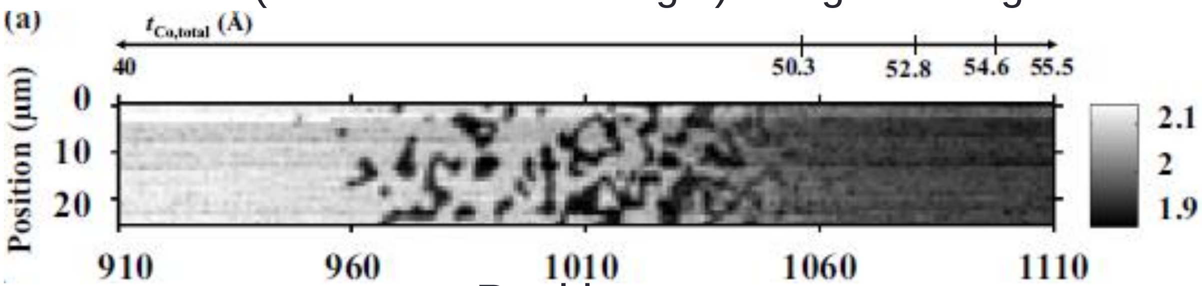

Position µm

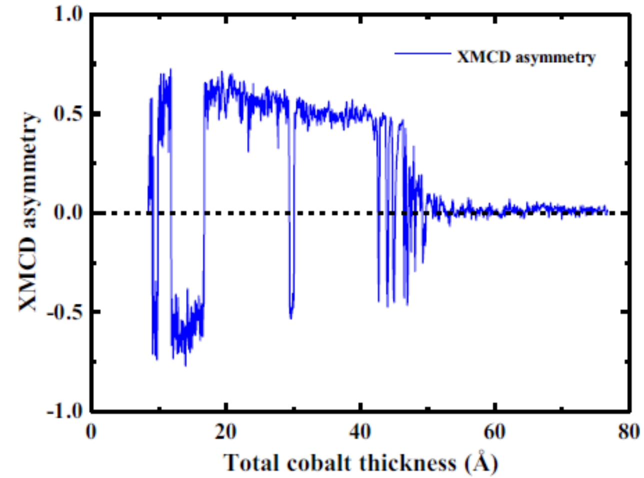

Large domains for thin Co, small domains for thicker Co

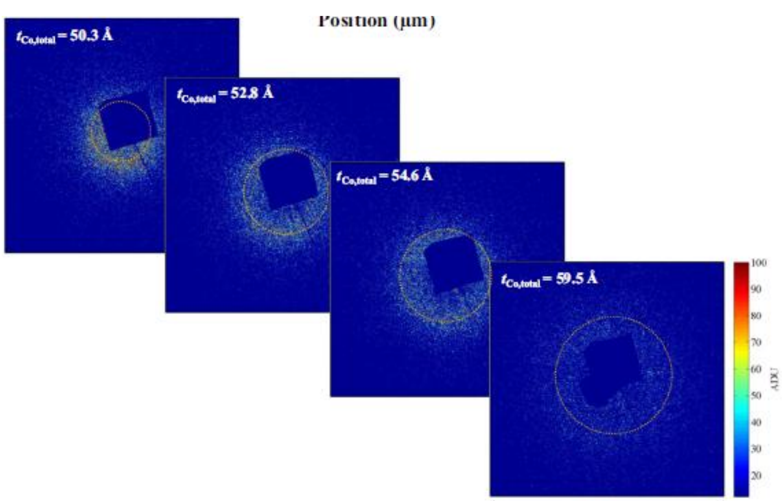

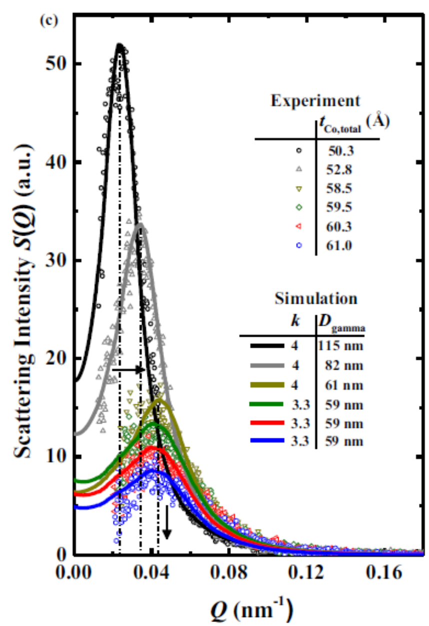

Good agreement between data and modeling!

Reduction of scattering intensity due to canting of magnetization

mSAXS of magnetic domain patterns

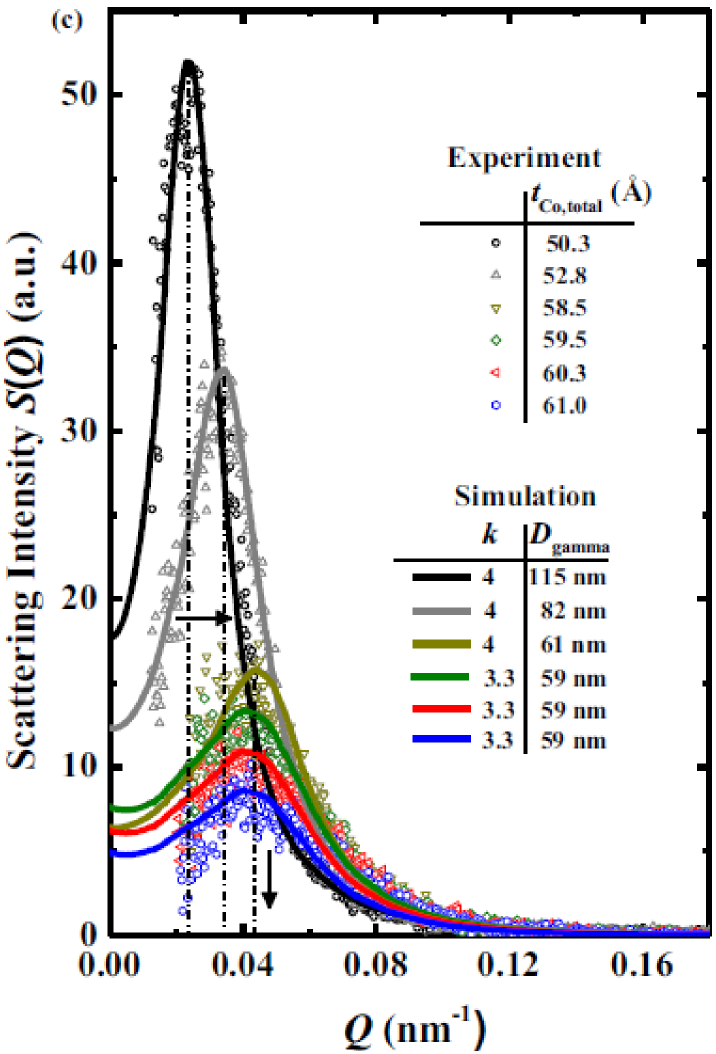

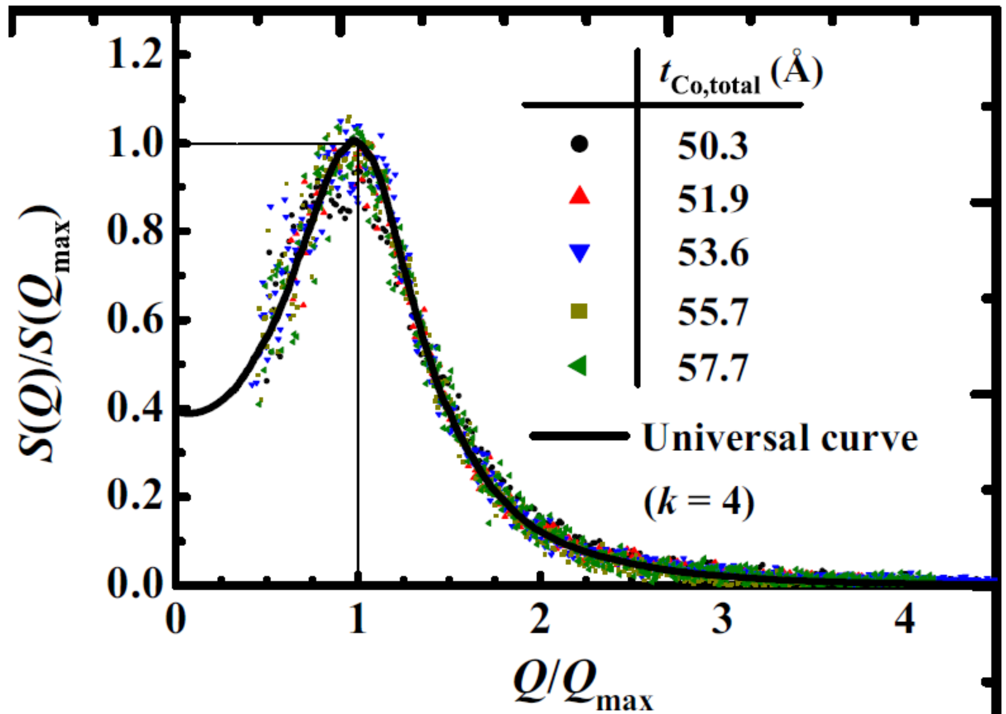

- While the effective domain width decreases with Co thickness, the (accessible) spatial domain size distribution stay the same as all curves can be normalized to one universal curve
- Higher order scattering peaks (additionally) suppressed due to broad size distribution

mSAXS of magnetic domain patterns

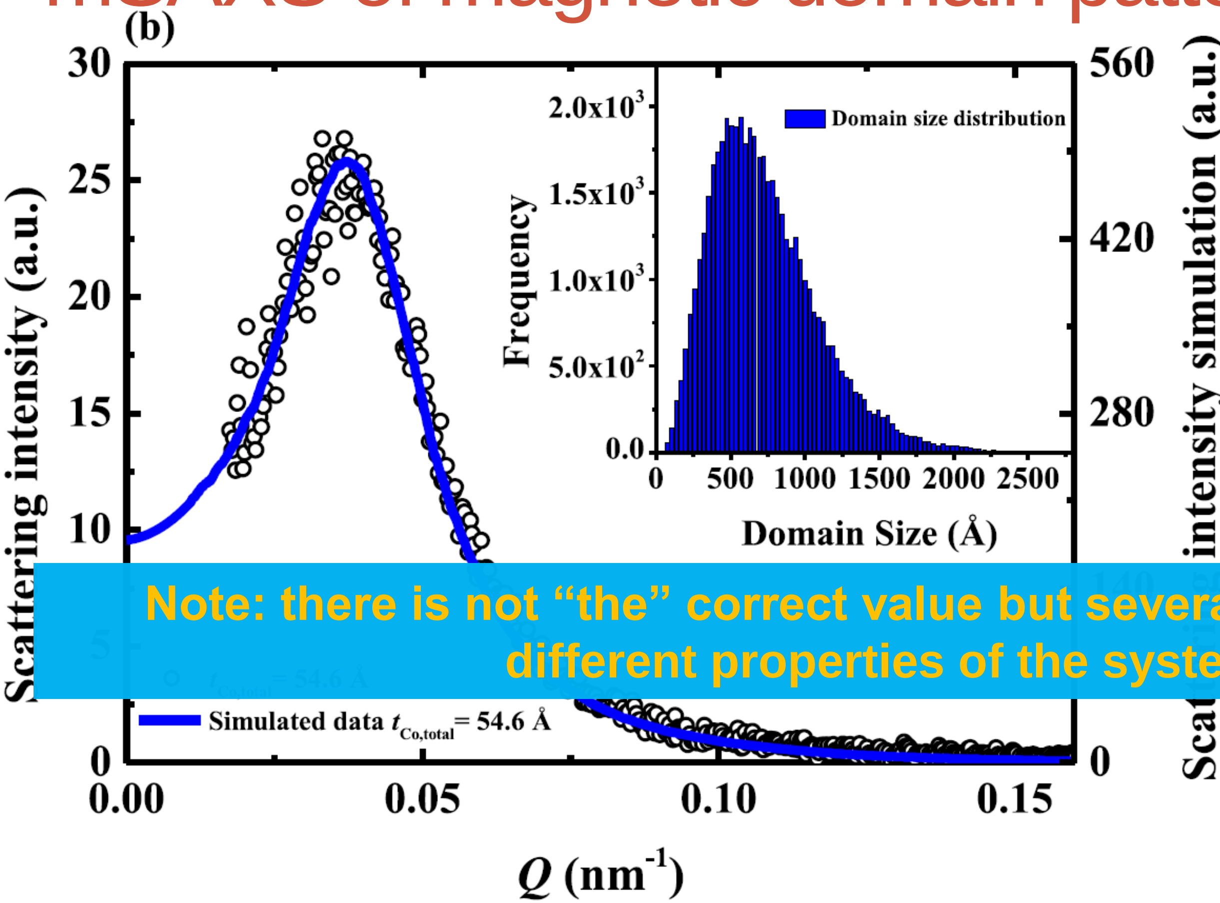

Note: there is not “the” correct value but several values reflecting different properties of the system!

Average domain width from scattering peak $D_{Q_{max}} = \frac{\frac{1}{2}2\pi}{Q_{max}} = 82.5\ \mathrm{nm}$

Average domain width from gamma distribution (deviation of 12.6%) $D_\gamma = k\vartheta = 73\ \mathrm{nm}$

mSAXS of magnetic domain patterns

(Most important) take-home messages:

- The magnetic scattering factor for circularly polarized light provides the absolute square of the Fourier transform of the magnetization pattern for the magnetization component || to the light‘s wave vector.
- For a 1D domain pattern **with equal size D of the up and down domains** and an infinitesimal small domain wall width, the first order of magnetic scattering is located at $2\theta = 2\arcsin\left(\frac{\lambda}{4D}\right)$; the scattering intensity of even orders are zero and the intensity of higher odd orders are much smaller than the one of the first order reflecting the q-dependence of the form factor of the magnetic unit cell.
- Finite domain wall widths further reduce the intensity of the higher orders.
- A domain size distribution can describe experimentally observed broad first order scattering peaks; the distribution further reduces the intensity of the higher orders.

Outline

Part III/2:

Studies on Magnetic Nanostructures

by André Philippi-Kobs (AP)

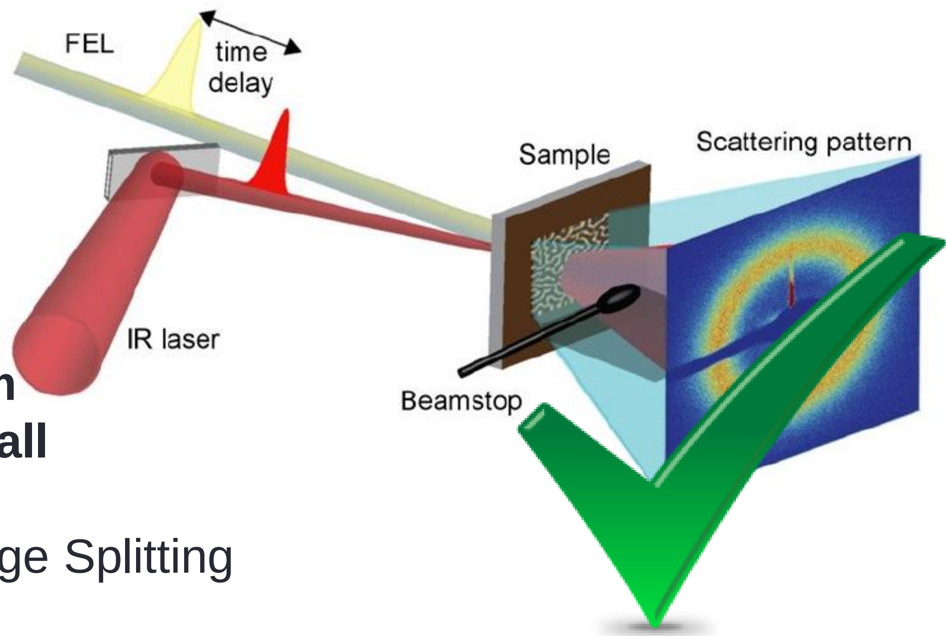

[29.6.] **X-ray Magnetic Circular Dichroism (XMCD) & Resonant Magnetic Small Angle X-ray Scattering (mSAXS)**

- Role of Spin-Orbit Coupling and Exchange Splitting
- Sum Rules
- XMLD and Natural Dichroisms
- mSAXS of Magnetic Domain Patterns